

Modelling for Loss Analysis of Inverter-fed Synchronous Machines

Samer Shisha and Chandur Sadarangani

School of Electrical Engineering, Electrical Machines and Power Electronics
 KTH (Royal Institute of Technology), Teknikringen 33, SE-100 44 Stockholm, Sweden
 Tel: (+46)-08 790 6168, E-Mail: samer.shisha@ee.kth.se

Abstract - This paper presents a novel method in which eddy current losses in a solid rotor direct torque controlled synchronous machine are found by utilizing a combination of analytical and FEM (Finite Element Method) simulations. The method is presented along with the results obtained. The article also briefly presents a new method in which 3D (three dimensional) current flows can be modelled using a 2D (two dimensional) FEM model.

I. INTRODUCTION

In the past few decades electrical machines have come to constitute one of the major consumers of electrical energy. This is particularly the case in industry, where in developed countries, the electrical energy consumed by electrical drives amounts to no less than 40% of the total amount produced [1].

The flexibility that inverter-fed drives provide in terms of speed and torque control makes them very attractive for various servo applications but also for other applications where high power output is required.

One control strategy, for electrical drives, that has become popular in recent years is the Direct Torque Control (DTC) Method. DTC was developed independently by German [2] and Japanese [3] researchers in 1980's.

There are many advantages that derive from using DTC [4], however one disadvantage is that it does not have a fixed switching frequency. This makes DTC difficult to model, in particular when using Finite Element Method (FEM) software in the analysis. The wide frequency spectrum that follows as a consequence of the variable switching frequency leads to losses in the machine that cannot be analysed using conventional methods.

The fact that the rotor is solid makes the analysis in that part of the machine more complicated. One of the major complications is the intricate harmonic interaction, as described in [5]. This is the reason for focusing on the analysis of the rotor in this study. Furthermore, by having a solid rotor, the eddy currents will produce the majority of the losses and hence it would be justified to concentrate on analysing these. It should also be noted that the majority of these losses, analysed here, are a direct consequence of the time harmonics in the signal.

II. DIRECT TORQUE CONTROL OPERATION

DTC is based on two widely accepted notions (according to [4] and [5]):

$$t_e \propto \psi_s \cdot \psi_r \cdot \sin(\delta) \tag{1}$$

$$\psi_s = \int (u_s - i_s R_s) dt \tag{2}$$

Where ψ_s and ψ_r are the time instantaneous stator and rotor flux linkages respectively and δ is the angle between the two vectors. R_s , u_s and i_s are the armature resistance, time instantaneous stator voltage and current respectively, while t_e is the time instantaneous electromagnetic torque. By choosing one of the six active voltage vectors and two zero vectors - available in a three phase machine as illustrated in Fig 1 - the flux linkage magnitude and position, and hence the torque, can be controlled.

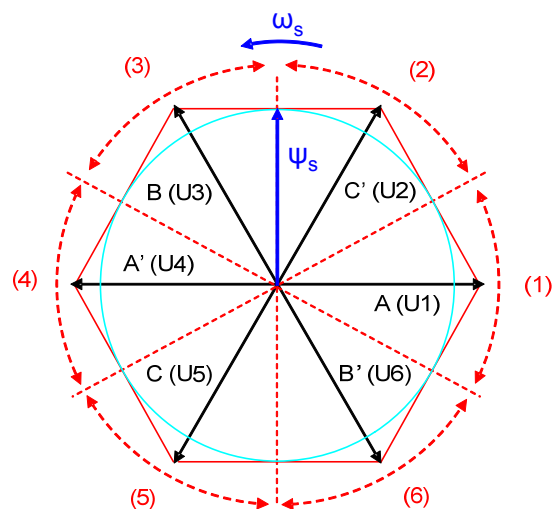


Fig 1. Voltage vectors and flux linkage paths in a DTC controlled machine.

It is the hysteresis control of the torque and flux linkage that causes the switching frequency to vary in a DTC system. By hysteresis control it is indicated that the voltage vector is only switched when it is necessary to change any of the two controlled parameters (torque and flux linkage in this case) back to their references. However it is possible to determine a range for the switching frequency by choice of appropriate

torque and flux linkage reference margins. The torque reference level is usually fixed while the flux linkage magnitude can be controlled as to obtain either circular or hexagonal paths around the airgap, such as those seen in Fig 1.

III. DTC MODELLING IN FEM

Today FEM modelling has become an almost integral part of machine design and analysis, as it provides a more economically viable, complementary solution to testing. FEM analysis also allows detailed aspects of the machine to be evaluated that would otherwise be impossible.

As mentioned earlier, the stochastic switching pattern of the DTC makes it inherently difficult to model in FEM software. Therefore it has been necessary to provide a more innovative approach for such modelling.

The method that is developed is based on obtaining the DTC switching signals, for the machine being analysed, from an analytical model and transferring the signals to the FEM software. As the models - analytical and FEM - are based on the same machine, the switching signals are representative for both. However some error is to be expected due to the difference in the two solving methods.

IV. ANALYTICAL MACHINE MODEL

The machine is modelled analytically using the conventional synchronous machine transient equations in the d-q reference frame which are given as follows:

$$\begin{bmatrix} v_{sd} \\ v_{sq} \\ v_{rd} \\ v_{rq} \end{bmatrix} = \begin{bmatrix} R_a & 0 & 0 & 0 \\ 0 & R_a & 0 & 0 \\ 0 & 0 & R_{rd} & 0 \\ 0 & 0 & 0 & R_{rq} \end{bmatrix} \begin{bmatrix} i_{sd} \\ i_{sq} \\ i_{rd} \\ i_{rq} \end{bmatrix} + p \begin{bmatrix} \psi_{sd} \\ \psi_{sq} \\ \psi_{rd} \\ \psi_{rq} \end{bmatrix} + \omega_{re} \begin{bmatrix} -\psi_{sq} \\ \psi_{sd} \\ 0 \\ 0 \end{bmatrix} \quad (3)$$

$$\begin{bmatrix} \psi_{sd} \\ \psi_{sq} \\ \psi_{rd} \\ \psi_{rq} \end{bmatrix} = \begin{bmatrix} L_{sd} & 0 & L_{ad} & 0 \\ 0 & L_{sq} & 0 & L_{aq} \\ L_{ad} & 0 & L_{rd} & 0 \\ 0 & L_{aq} & 0 & L_{rq} \end{bmatrix} \begin{bmatrix} i_{sd} \\ i_{sq} \\ i_{rd} \\ i_{rq} \end{bmatrix} + \begin{bmatrix} \psi_f \\ 0 \\ \psi_f \\ 0 \end{bmatrix} \quad (4)$$

$$\begin{bmatrix} L_{sd} \\ L_{sq} \\ L_{rd} \\ L_{rq} \end{bmatrix} = \begin{bmatrix} L_{ad} + L_{ls} \\ L_{aq} + L_{ls} \\ L_{ad} + L_{lrd} \\ L_{aq} + L_{lrq} \end{bmatrix} \quad (5)$$

Where v_s and i_s are the instantaneous stator voltage and current components, while v_r and i_r are the rotor equivalents. R_a is the armature resistance, R_r is the sub-transient resistance. L_s is the stator synchronous inductance while L_r is the rotor sub-

transient inductance. L_{ls} is the stator leakage inductance and L_{lr} is the rotor sub-transient leakage inductance. The flux linkage due to the field winding is represented by ψ_f . The differentiation operator is represented by p , while ω_{re} is the electrical speed of the rotor. The d- and q-axis are indicated by the equivalent letter subscript extensions, if applicable, for each of the components respectively.

The solid pole-plate is assumed to shield the field winding from the high frequency harmonics in the signal. Therefore the model neglects the effects of the transient impedance. The effect of the currents induced in the solid pole-plates is accounted for by the sub-transient impedance, the value of which is obtained from the FEM model using the method described in the next section.

V. OBTAINING SUB-TRANSIENT IMPEDANCE

The value of the sub-transient impedances are usually obtained using various testing procedures, such as those described in [6]. In the research presented in this article, however, FEM modelling is used to obtain the sub-transient impedances to be utilised in the analytical model of the machine. This method utilises two simulations, one for the d-axis and another for the q-axis.

For the d-axis, the rotor is aligned with the axis of the armature phase, where the latter is fed from a high frequency current source. The high frequency stator current induces currents in the rotor pole-plate in the same manner as the time harmonics. The frequency used is that of the highest harmonic frequency being considered in the evaluation.

Consider the equivalent circuit of the synchronous machine in the d-axis, seen in Fig 2 (a), where the d-axis of the rotor is aligned with the phase axis (phase A in this case). Phase A is fed from the sinusoidal current source at a high frequency, while the other two phases are open circuited.

By evaluating the voltage across the phase terminals it is possible to calculate the value of the sub-transient impedance using:

$$Z_{rd} = \left[\frac{1}{Z_{tot} - j\omega_h L_{ls} - R_s} - \frac{1}{j\omega_h L_{ad}} \right]^{-1} \quad (6)$$

$$Z_{tot} = \frac{V_d}{I_s} \quad (7)$$

$$Z_{rd} = R_{rd} + j\omega_h L_{lrd} \quad (8)$$

Where ω_h is the frequency of the current, Z_{tot} is the total impedance seen at the terminals of the phase and Z_{rd} is the sub-transient impedance in the d-axis.

This procedure is then repeated for the q-axis where the rotor d-axis is moved 90° electrical, aligning the rotor q-axis with the phase axis. These calculated sub-transient impedance values are subsequently inserted into the analytical machine model.

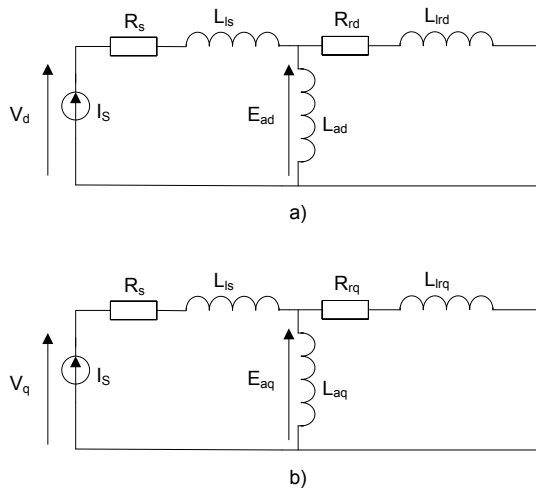


Fig 2. Equivalent circuit of a synchronous machine with damper windings, neglecting the transient impedance, a) in the d-axis and b) in the q-axis.

VI. ANALYTICAL DTC MODEL

The general block diagram of a DTC system coupled to the machine is shown in Fig 3. The block named “Optimal Switching Table Selector” consists basically of a lookup table such as the one given in TABLE 1, which is also used in this analysis.

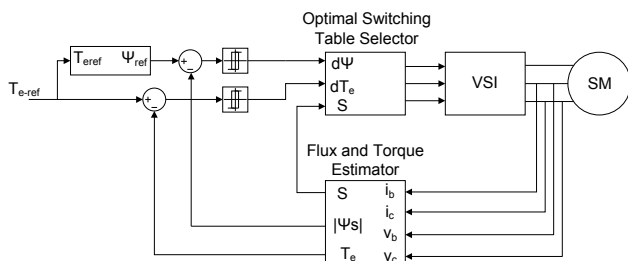


Fig 3. General block diagram of a DTC system.

The selection from the table depends on the status of the torque and flux linkage as well as the sector position of the flux linkage vector. The sectors are defined as the crested arrows shown in Fig 1, where each sector spans 60° electrical with the centre coinciding with the corresponding voltage vector.

TABLE 1
DTC OPTIMAL SWITCHING TABLE.

DΨ	DT	Sect. 1	Sect. 2	Sect. 3	Sect. 4	Sect. 5	Sect. 6
1	1	U2	U3	U4	U5	U6	U1
	-1	U6	U1	U2	U3	U4	U5
-1	1	U3	U4	U5	U6	U1	U2
	-1	U5	U6	U1	U2	U3	U4

A circular flux linkage path is used in this model, where the flux linkage reference is held constant around the perimeter of the machine. The flux reference is calculated in this case assuming zero d-axis current, with the field current held constant, using the following equation:

$$|\psi_s| = \sqrt{\psi_f^2 + \left(L_{aq} \frac{2 \cdot T_{ref}}{3 \cdot pp \cdot \psi_f} \right)^2} \quad (9)$$

Where pp is the number of pole-pairs of the machine and T_{ref} is the electromagnetic torque output required.

VII. DTC OPERATION RESULTS

A. Torque and Flux Linkage

The switching signals obtained from the analytical simulation of the DTC system, presented above, are inserted into the FEM software in order to emulate the DTC operation therein. The simulation is carried out using a torque reference level of approximately 0.88 p.u. and the flux linkage reference is calculated, using (9), to approximately 0.94 p.u.

The torque obtained from the FEM model and that obtained from the analytical equivalent are plotted and compared in Fig 4. It is clear from the plots that the torque results obtained from the two models are similar. However, the torque dips in the FEM model are slightly larger than those obtained from the analytical equivalent, but that is acceptable considering the difference in the solving methods.

The stator flux linkage plots obtained from the two models are given in Fig 5, where it is clear that the two plots are nearly identical.

B. Pole-plate Losses

The high number of harmonics in the DTC signal lead to induction of currents in the solid rotor as was mentioned earlier. These induced currents lead to consequent time harmonic losses. Due to the high frequency of these harmonics, the induced currents will be mainly constrained to the top layer of the rotor pole-plates. This is a direct consequence of the skin effect, which restricts the current incursion into the material to a narrow depth.

The total losses evaluated on the pole-plate amount to approximately 0.11 p.u. of the rated input power. The majority of these are directly related to the inverter time harmonics. A small portion of these pole-plate losses, around 7% in this case, are due to the slotting harmonics.

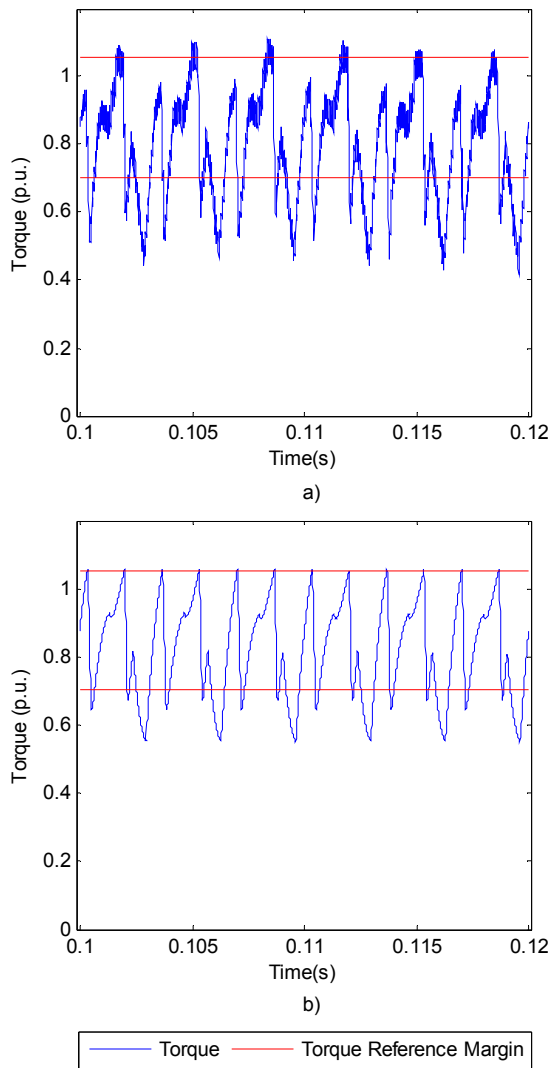


Fig 4. Torque obtained from a) FEM simulation and b) the equivalent analytical simulation.

As the pole-plate losses depend on the induced current it is useful to analyse this current. Fig 6 shows the total integrated current in one pole-plate of the machine. It is found that the pole-plate current is repetitive at six times the stator frequency, which allows evaluation of the current over 1/6th of the machine period. This can also be verified by looking at the armature current frequency spectrum, seen in Fig 7, where it is clear that the 5th and 7th harmonics are the most prominent and the lowest order of the harmonic components (apart from the fundamental). These combine and transform to the 6th on the rotor side.

Furthermore it is also useful to compare the magnitude of the frequency harmonics in the pole-plate current to those expected. The expected magnitude is calculated using the power superposition method presented in [5]. From Fig 7 it is obvious that the most significant stator harmonics are the 5th, 7th, 11th, 13th, 17th and 19th. These transform to the 6th, 12th and

18th on the rotor side, when considering their direction of rotation with respect to the rotor along with their frequency.

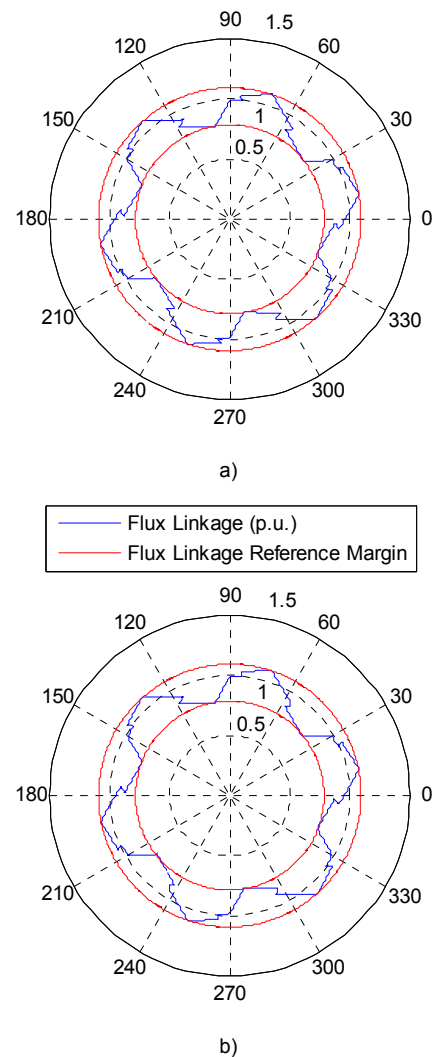


Fig 5. Stator flux linkage vector magnitude vs. position, obtained from a) FEM simulation and b) analytical simulation.

The expected magnitude according to the power superposition method is calculated using (10), for each component.

$$\begin{aligned}
 I_{R6} &= \sqrt{I_{S5}^2 + I_{S7}^2} \\
 I_{R12} &= \sqrt{I_{S11}^2 + I_{S13}^2} \\
 I_{R18} &= \sqrt{I_{S17}^2 + I_{S19}^2}
 \end{aligned}
 \tag{10}$$

Where I_R and I_S are the rotor pole-plate and stator current harmonic components respectively, each followed by the equivalent harmonic number of the component in question.

This analysis, however, accounts only for the losses in the pole-plate of the rotor. In order to obtain the total rotor losses we need to consider the current flow on the rotor body.

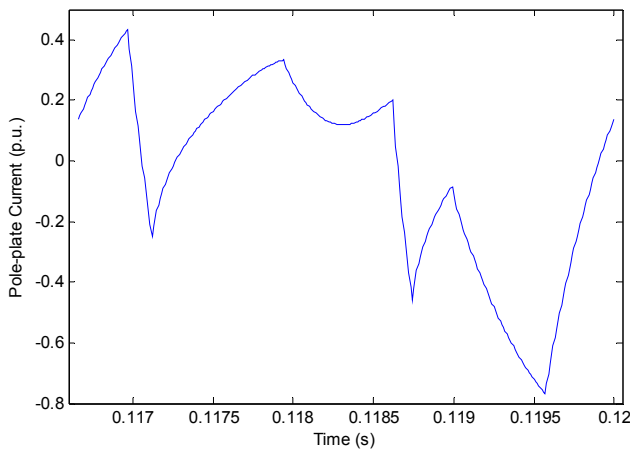


Fig 6. Pole-plate current obtained from the FEM model.

Comparing the expected and actual current harmonics on the pole-plate, see Fig 8, it is possible to note that the power superposition method does not yield accurate results. The actual pole-plate current harmonics magnitude are not equal to those expected using the superposition method.

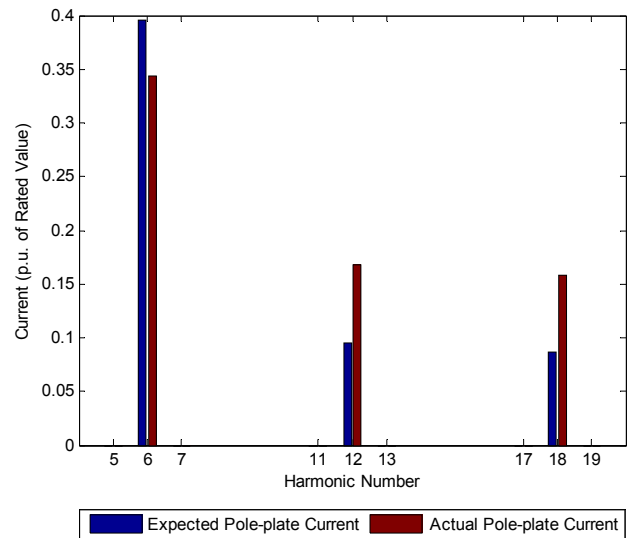


Fig 8. Expected vs. the actual current harmonics on the pole-plate of the FEM model.

VIII. POLE-PLATE COUPLING METHOD

As the rotor is solid the current flow will be 3D (three dimensional), with a flow path that depends on the flux linkage harmonics that induced the current. This means that there will be current components that flow in the pole-plate itself, as shown in Fig 9 (a), as well as components that will flow from one pole to the next through the rotor body, Fig 9 (b). These current components flowing in the rotor body flow tangentially to the direction of rotation. In 2D (two dimensional) FEM analysis this tangential current component will not be accounted for.

In order to be able to analyse this current using 2D FEM and simplify the analysis, a novel method has been developed. In this method, two consecutive pole-plates are coupled through an external impedance representing the impedance of the rotor body, as is seen in Fig 10.

In the previous FEM simulation only one pole of the rotor was simulated, using anti-symmetric boundary conditions, automatically setting the current in the next pole-plate equal in magnitude but opposite in direction to the one being simulated. This is equivalent to setting the inter-polar impedance value equal to zero.

When altering the inter-polar impedance to a finite value, the losses in the pole-plate are also expected to change as the current in the q-axis is restricted. What is needed is an indication of the significance of these inter-polar currents on the pole-plate losses.

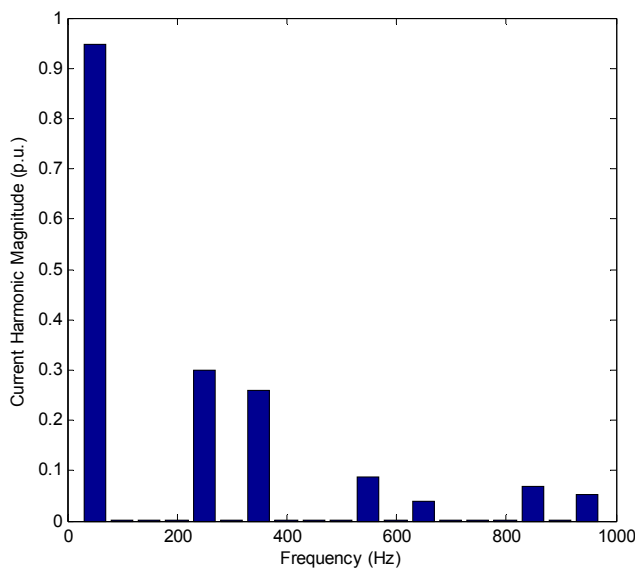


Fig 7. Armature current spectrum, obtained from the FEM model.

This difference between the actual and calculated values of pole-plate current harmonics verifies that the evaluation of pole-plate losses on the solid rotor of synchronous machines is not straight forward to calculate using the power superposition method. An accurate analysis entails the use of FEM in order to get a correct insight of what is actually taking place on the rotor.

IX. CONCLUSION

In this article a novel method is presented with which the eddy current losses in the pole-plates of an inverter driven solid rotor synchronous machine are analysed using 2D FEM (Finite Element Method) software. The emphasis has been placed on Direct Torque Control application. Furthermore the effect of the inter-polar current on the pole-plate losses is evaluated using a complementary method in which two consecutive poles of the rotor are coupled through an external circuit in the FEM model. The advantage of this cross coupling method is the fact that it is applicable using 2D FEM, hence avoiding the need for 3D FEM.

The presented methods are not restricted in any way to synchronous machines, rather they offer a wide range of opportunities for applications where other machine types and control methods are involved.

X. MACHINE DATA

The following are the name plate data of the simulated machine:

Synchronous Machine 3 Phase AC
 50 Hz
 230 V, 10.8 A
 7.5 kVA, Power Factor = 0.85 (Cap)
 Field Winding: 1.9 A
 4 Pole

REFERENCES

- [1] Chandur Sadarangani, *Electrical Machines – Design and Analysis of Induction and Permanent Magnet Machines*, Royal Institute of Technology 2000.
- [2] M. Depenbrock, *Direkte Selbstregelung (DSP) für Hochdynamische Drehfeldantriebe mit Stromrichterspeisung*, ETZ-Archiv, Bd. 7, H. 7, 1985.
- [3] I. Takahashi and T. Noguchi, *A new Quick Response and High Efficiency Control Strategy of an Induction Motor*, IEEE IAS Annual Meeting 1985.
- [4] Peter Vas, *Sensorless Vector and Direct Torque Control*, Oxford University Press 1998.
- [5] Samer Shisha and Chandur Sadarangani, *Analysis of Losses in Inverter Fed Large Scale Synchronous Machines using 2D FEM Software*, PEDS 2007 Conference Proceeding.
- [6] IEEE Guide: *Test Procedures for Synchronous Machines*, IEEE Std 115-1995(R2002).

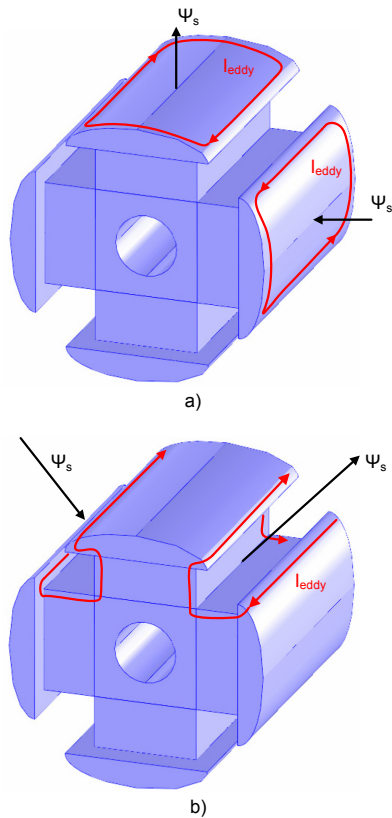


Fig 9. Illustration of the solid rotor of a synchronous machine a) showing the current flow in the pole-plate and b) showing the cross-pole current.

By setting the inter-polar impedance to a high value it is possible to restrict the inter-polar currents to nearly zero.

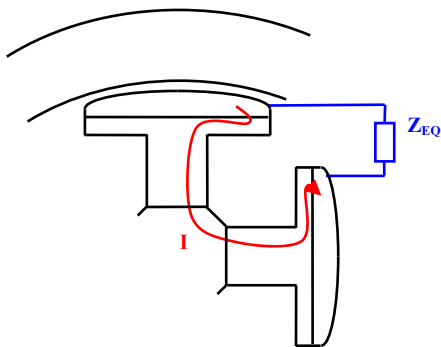


Fig 10. Cross-pole coupling model used to account for the cross-pole currents.

What is found is that the total pole-plate losses (including the slot-harmonic losses) reduce to 0.09 p.u. of the rated input power. This can be compared to the 0.11 p.u. when using a value equivalent to zero for the cross-pole impedance in the FEM simulation. This is an indication that the effect of the value of the inter-polar impedance on the pole-plate losses is small.